Viscosity of surfactant stabilized emulsions

K. M. B. Jansen,[a)] W. G. M. Agterof, and J. Mellema

*Department of Applied Physics, University of Twente, P.O. Box 217,
7500 AE Enschede, The Netherlands*

Synopsis

A new scaling parameter for the viscosity of surfactant stabilized emulsions is proposed. We suggest that the attractive force between emulsion droplets is caused by the small surfactant micelles in the continuous phase of an emulsion. The new scaling parameter will be referred to as the depletion flow number, $Fl_d = 4\pi\eta_s\dot{\gamma}a^2a_m/kT\phi_m$, and is defined as the ratio between the viscous energy needed to separate the droplets and the depletion energy that opposes this separation. Here η_s, a, a_m, and ϕ_m are the solvent viscosity, dispersed phase droplet radius, micelle radius, and micelle volume fraction, respectively. Fl_d is of the order of unity at the onset of shear thinning and is capable of explaining all previously observed effects of drop size, solvent viscosity, and surfactant concentration. With master curves which are obtained by using Fl_d as the running parameter, a relatively simple empirical model is constructed which can reproduce the viscosity curves of many previously reported in the literature. © *2001 The Society of Rheology.* [DOI: 10.1122/1.1410372]

I. INTRODUCTION

Emulsions are dispersions of two immiscible liquids such as oil and water which find application in a wide range of industries including chemical engineering, food processing, pharmaceutical manufacturing, and enhanced oil recovery. In order to increase their stability, a small amount of surfactant (emulsifier) is added to the continuous phase. If the surfactant concentration is above the critical micelle concentration (CMC), surfactant aggregates, or micelles, form. Emulsions with an excess amount of surfactant can therefore be regarded as a dispersion of large, micron sized, fluid droplets surrounded by a continuous phase with small (nanometer sized) micelles. Aronson (1989) studied unstable emulsion systems and concluded that the flocculation and creaming observed could be caused by micelle depletion effects in the gap between two emulsion droplets. This is analogous to the effect of nonadsorbed polymers on colloid stability [Asakura and Oosawa (1958)]. Aronson then showed that the associated free energies are in excess of several kT. This idea of micelle depletion induced creaming was used by Bibette (1991) to separate emulsions by drop size, resulting in nearly monodisperse emulsions. Other surfactant induced effects were observed by Pal (1993) who explained the observed viscosity changes by surfactant-induced inhibition of internal circulation. The same author studied the depletion effect caused by polymer additives on the viscosity of emulsions [Pal (1992, 1993)]. This article however is, to the best of our knowledge, the first first detailed study in which micelle-induced depletion forces are used to scale the emulsion viscosity.

[a)]Author to whom all correspondence should be addressed; electronic mail: k.m.b.jansen@wbmt.tudelft.nl

The purpose of this article is twofold. First, we will introduce a new scaling parameter based on micelle depletion interaction and show that this parameter is capable of explaining previously observed dependencies of the surfactant concentration, droplet radius, and solvent viscosity. The second purpose is to provide a simple empirical model for the emulsion viscosity. This model may prove useful both as a reference for future viscosity measurements and as a tool for the design of processing equipment.

II. PREVIOUS WORK

Although many viscosity studies of all kinds of emulsions are reported in literature, only a small minority of them actually deals with a search for a physical interpretation [e.g., Otsubo and Prud'homme (1994a); Pal (1997); Princen and Kiss (1989)]. There is general agreement in the literature that the shape of the viscosity curves is similar to those of suspensions of solid particles: a shear rate independent viscosity at low shear rates (if yield stress is absent), a shear thinning region, and a high shear plateau. This behavior is captured with the modified Cross equation:

$$\eta_r = \eta_{r,\infty}(\varphi,\lambda) + \frac{\eta_{r,0}(\varphi,\lambda) - \eta_{r,\infty}(\varphi,\lambda)}{1 + (k'\dot{\gamma})^m} + \frac{\tau_y}{\eta_s\dot{\gamma}}, \tag{1}$$

where the relative viscosity $\eta_r = \eta/\eta_s$ is the ratio between the emulsion viscosity and the solvent viscosity, φ stands for the dispersed phase volume fraction, and $\lambda = \eta_d/\eta_s$ is the ratio between the viscosity of the dispersed phase and the solvent. The subscripts "∞" and "0" refer to the high shear and low shear plateaus, respectively. The coefficient m in the second term corresponds to the slope of the viscosity curve in the shear thinning region and it is usually close to 0.8. The yield stress term [the last term in Eq. (1)] will be discussed later. The onset of shear thinning is determined by the value of k' and it is this parameter which is of physical interest for understanding of the shear thinning region. Since $k'\dot{\gamma}$ is dimensionless, the parameter k' has the dimension of time and must be a combination of system variables like the droplet radius a, the solvent viscosity η_s, the density ρ_s, and surfactant properties like the interfacial tension σ. It is evident that the disruptive force is due to viscous friction but the origin of the cohesive force is not yet clear.

For a suspension of hard colloidal particles (with radius $a < 1\ \mu$m) it turned out that the competition between the Brownian and hydrodynamic forces determines the flow behavior. Krieger (1972) showed that the Peclet number $Pe = \eta_s\dot{\gamma}a^3/kT$ was the appropriate scaling parameter for the viscosity. For larger particles like emulsion droplets ($a \sim 10\ \mu$m) the Brownian force becomes negligibly small and a different explanation for the flow behavior is needed. A natural choice for a dimensionless parameter in emulsions is the ratio between the viscous force and interfacial tension force, known as the capillary number: $Ca = \eta_s\dot{\gamma}a/\sigma$. This scaling parameter is used for modeling the viscosity of foams [or highly concentrated emulsions, Princen and Kiss (1989); Reinelt and Kraynik (1989)] and in simulations of emulsion flow [see e.g., Loewenberg and Hinch (1996)]. The problem is that all experiments on emulsions show scaling proportional to $\sim \dot{\gamma}a^2$ [Pal (1996, 1997); Otsubo and Prud'homme (1992, 1994a, 1994b)], which does not match that of the capillary number ($\sim \dot{\gamma}a$) nor that of the Peclet number ($\sim \dot{\gamma}a^3$). Otsubo and Prud'homme (1992, 1994a, 1994b) performed an extensive set of measurements on systems in which they systematically varied the dispersed phase volume fraction (between 10% and 90%), the average drop radius (between 4.5 and 12 μm), and the solvent viscosity (between 2.65 and 660 mPa s). In all cases they found that scaling of $\sim \dot{\gamma}a^2$ (or $\sim \dot{\gamma}a^2/\sigma$ as they claim) caused individual viscosity curves to

overlap. Pal (1996) showed that $\dot{\gamma}a^2$ scaling holds even if the drop size varies by more than an order of magnitude. In an attempt to explain his results he proposed the particle Reynolds number as the only possible dimensionless number with the required $\dot{\gamma}a^2$ scaling: $Re_p = \rho_s\dot{\gamma}a^2/\eta_s$, which is the ratio between inertia and viscous forces. The problem here is that at the onset of shear thinning the inertia force is typically six orders of magnitude smaller than the viscous force [cf. Pal (1997)] and is thus not likely to be the true scaling parameter. Note that the Re_p number scales *inversely* proportional to the solvent viscosity while the other dimensionless numbers scale as $\eta_s\dot{\gamma}$. Unfortunately no studies are available in which the solvent viscosity was changed systematically while keeping all other parameters (including the viscosity ratio) constant.

III. NEW SCALING HYPOTHESIS

In the following we will propose a new and completely different physical explanation for viscosity scaling. In our view the attractive force between the relatively large fluid droplets is due to depletion effects caused by the much smaller surfactant molecules and micelles. According to Asakura and Oosawa theory (1958) the depletion energy in the limit of $a/a_m \neq 1$ is given as $E_{\mathrm{depl}} \cong \frac{3}{2}kT\phi_m a/a_m$ where a_m and ϕ_m stand for the micelle (or coiled surfactant) radius and volume fraction, respectively. The viscous energy needed to overcome this attraction energy is given by the viscous friction force multiplied by the distance over which the force must be applied to ensure breakage. In shear flows this distance scales proportionally to a, thus $E_{\mathrm{visc}} = 6\pi\eta_s\dot{\gamma}a^3$. This then results in a new dimensionless number which will be referred to as the depletion flow number,

$$Fl_d = \frac{4\pi\eta_s\dot{\gamma}a^2 a_m}{kT\phi_m}.$$

(2)

The new scaling parameter should apply in the region where Brownian forces are small (this condition is usually fulfilled for emulsions with drop sizes above 1 μm) and where the dispersed phase fraction is below the close packing limit (about 0.70). Above this limit the droplets are deformed and different scaling behavior is expected. In this article we will focus on emulsions in which the surfactant is present in the form of micelles. It is, however, also of interest to consider the depletion flow number during micelle formation. Below the CMC surfactant molecules are present as coiled molecules with dimensions of 1 nm typically. During micelle formation about 100 of these molecules form a single micelle with a radius of, say, 3 nm. The scaling parameter Fl_d which is proportional to the ratio α_m/ϕ_m will thus increase by a factor of 10 during micelle formation (assuming that all surfactant molecules convert into micelles). This means that just below the CMC depletion effects are even stronger and may lead to unexpected aggregation effects.

The depletion flow number just introduced has the $\eta_s\dot{\gamma}a^2$ scaling observed in the experiments and predicts a shift of the viscosity curves towards lower shear rates if the micelle concentration increases or the micelle size decreases. Such surfactant concentration effects have sometimes been reported in the literature. Here we consider the measurement set of Suzuki *et al.* (1969) for water in cyclohexane ($+CCl_4$) emulsions stabilized with Arlacel 60 (sorbitan monostearate) surfactant. As shown in Figs. 1(a) and 1(b) the viscosity curves indeed superpose when plotted against the depletion flow number. The only exception appears to be the curve for the highest surfactant concentration which is slightly higher than the rest.
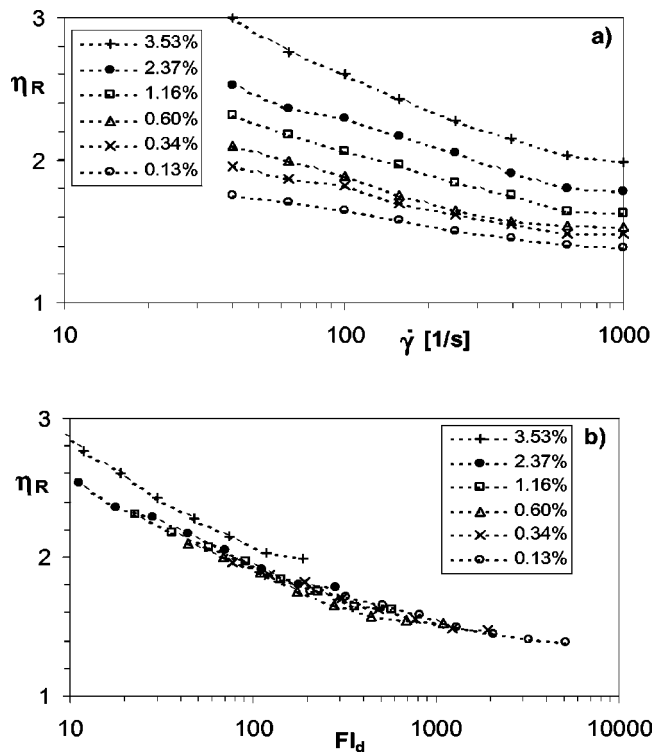
FIG. 1. Effect of surfactant concentration for a water in cyclohexane emulsion. (a) Relative emulsion viscosity vs shear rate. (b) Relative viscosity vs depletion flow number. The numbers refer to the volume fractions of surfactant (Arlacel 60). The droplet volume fraction and size were $\varphi = 0.15$ and $a_{32} = 1.5 \ \mu$m, respectively.

The use of the depletion flow number as defined above requires not only knowledge of the micelle volume fraction but also that of the micelle size. The micelle volume fraction follows from the micelle density and the *excess* surfactant concentration (i.e., the amount of surfactant in excess of the CMC plus the amount of adsorbed surfactant). The amount of adsorbed surfactant can be estimated from the area per surfactant molecule (typically 40 Å^2) and is usually small (< 0.05 wt %). For scaling purposes the micelle density can be taken as that of the surfactant density or, even more crudely, equal to that of the aqueous phase (~ 1.0 g/l). The micelle size is a much more difficult parameter to estimate. For nonionic surfactants which consist of an aliphatic chain of n units and a polyethyleneoxide part of m units (abbreviated C_nE_m), however, empirical relations are available. Commercially available examples of this class of surfactants are Neodol, Dobanol, and Brij. The critical micelle concentration of these products is reproduced well by the empirical relation [see, e.g., Huibers *et al.* (1996)]

$$\log_{10} \text{CMC} = 1.646 - 0.496n + 0.0437m \quad (\text{CMC in mole/1}). \tag{3}$$

In addition, the micelle size data for C_nE_m surfactants can be approximated as (see Table I)

$$a_m = 16.3 + 0.59n + 0.73m \quad (\text{in Å}). \tag{4}$$

For surfactants for which no micelle data are available, the length of the apolar chain,

$$l_{\text{chain}} \approx 1.5 + 1.265n \quad [\text{in Å; Tanford (1980)}], \tag{5}$$

TABLE I. Micelle properties of commonly used surfactants.

Surfactant	Alternate name	Cont. phase	a_m (Å)	N^{aggr}	CMC[a] (mole/l)	Source
Polytheleneglycol (...)phenylether	Triton X-100	Water	44 ± 1	80–100	9.0×10^{-4}	Streletzky and Phillies (1995), Phillies and Yambert (1996)
Sodium dodecylsulfate	SDS	Water	18	60	0.0081	Forland et al. (1998)
Sodium decylsulfate	SdeS, Alipal CD-128	Water		50	0.032	Shinoda et al. (1963)
Cetyltrimethyl ammonium bromide	CTAB	Water	~ 50	90	9.2×10^{-4}	Mondain-Monval et al. (1995)
$H(CH_2)_{10}(C_2H_4O)_8$	$C_{10}E_8$	Water	26	52	0.001	Sato et al. (1988)
$H(CH_2)_{12}(C_2H_4O)_6$	$C_{12}E_6$	Water	28.8	103	6.8×10^{-5}	Penfold et al. (1997)
$H(CH_2)_{12}(C_2H_4O)_6$	$C_{12}E_6$	80% ethyl glycol	28.5	128		Penfold et al. (1997)
$H(CH_2)_{12}(C_2H_4O)_6$	$C_{12}E_6$	Benzene	10	1.2		Ravey et al. (1984)
$H(CH_2)_{12}(C_2H_4O)_8$	$C_{12}E_8$	Water	28	62	7.1×10^{-5}	Sato et al. (1988)
$H(CH_2)_{12}(C_2H_4O)_{23}$	$C_{12}E_{23}$, Brij 35	Water	39.5	56	9.1×10^{-5}	Shinoda et al. (1963)
$H(CH_2)_{14}(C_2H_4O)_8$	$C_{14}E_8$	Water	29	81	9×10^{-6}	Sato et al. (1988)
Sodium ethylhexyl sulfosuccinate	AOT	Isooctane	20	43	$\sim 6 \times 10^{-4}$	Amararene et al. (2000)
Sorbitan monooleate	Span 80, Emsorb 2500	Dodecane	25	3–20		Abou-Nemeh and Bart (1998)
Sorbitan monostearate	Arlacel 60	Benzene		113	2.3×10^{-3}	Schick (1967)

[a]The CMC values are taken from Schick (1967) and from Rosen (1989).

may serve as an initial estimate of the micelle size. It should be noted that at high surfactant concentrations some micelles loose their spherical shape and form cylindrical or lamellar structures [Glatter et al. (2000)]. It is obvious that in those cases Eq. (2) ceases to be valid. In Table I we present the micelle sizes of some of the more commonly used surfactants. It then becomes clear that micelle radii are typically about 30 Å, which is three to four orders of magnitude smaller than the size of the emulsion droplet. Moreover, the variation in micelle size turns out to be relatively small, certainly in comparison with possible variations in most of other depletion flow number variables.

In summary, the observed scaling with η_s, $\dot{\gamma} a^2$, and ϕ_m^{-1} is strong evidence for the depletion flow number as a dimensionless shear thinning parameter.

IV. DEVELOPMENT OF A GENERAL EMULSION VISCOSITY MODEL

A. The viscosity model

In Sec. III it was shown that the depletion flow number, Fl_d, is the proper parameter which governs the shear thinning part of the emulsion viscosity curve. Rewriting Eq. (1) then results in

$$\eta_r = \eta_{r,\infty}(\varphi,\lambda) + \frac{\eta_{r,0}(\varphi,\lambda) - \eta_{r,\infty}(\varphi,\lambda)}{1 + kFl_d^m} + \frac{\tilde{\tau}_y(\varphi,\lambda)}{Ca}, \tag{6}$$
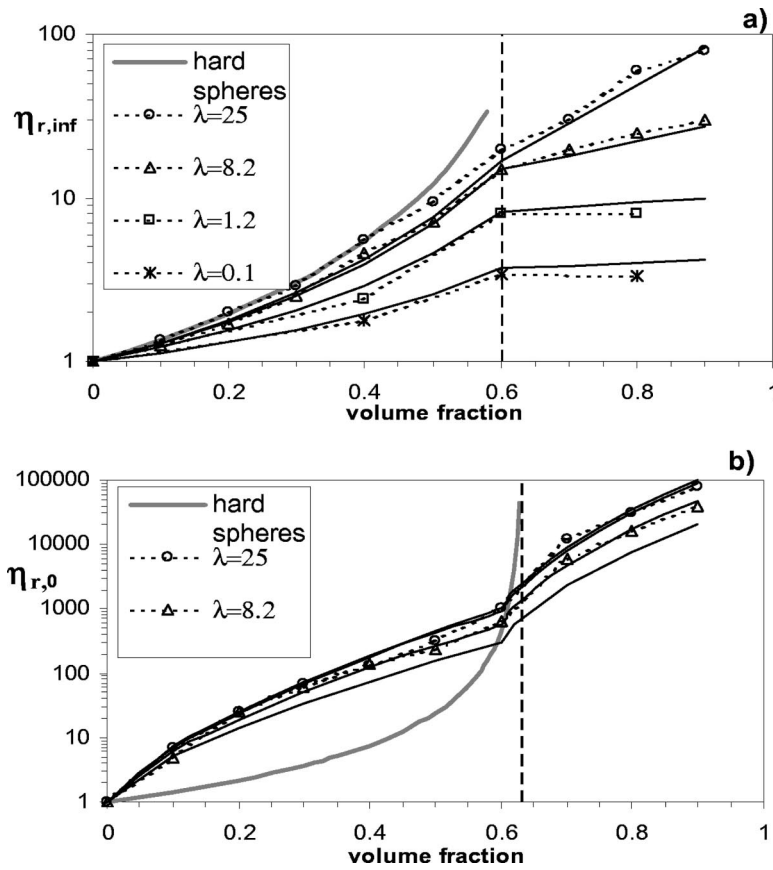
FIG. 2. Effect of volume fraction and viscosity ratio on (a) high shear viscosity and (b) low shear viscosity. The thin solid lines are correlation functions given by Eqs. (4) and (5) and the thick gray line is the hard sphere limit.

where the yield stress is put in dimensionless form: $\tilde{\tau}_y = \tau_y a/\sigma$. Our next task is to find expressions for functions $\eta_{r,\infty}$, $\eta_{r,0}$, and $\tilde{\tau}_y$ as well as for parameters k and m. In doing so, we will restrict ourselves to the part of the viscosity curve where the drop size is constant and breakup does not occur. Note that the shear rate at which breakup occurs depends on the volume fraction as well as on the viscosity ratio [Jansen *et al.* (2001)]. First we will focus on the viscosity plateau values, $\eta_{r,\infty}(\varphi,\lambda)$ and $\eta_{r,0}(\varphi,\lambda)$. We therefore use the extensive data set of Otsubo and Prud'homme (1992, 1994a, 1994b) and replot their viscosity curves with Fl_d as the running variable. In that way the curves for different drop sizes are superimposed and master curves for each combination of φ and λ are constructed. From these master curves the plateau values were estimated and are shown in Fig. 2. As a comparison the limiting case for solid particles is shown as the thick gray line. For the high shear viscosity case [Fig. 2(a)] the situation is as expected. The emulsion viscosity shifts upwards with an increase in the viscosity ratio and the hard sphere limit is approached for the data set with $\lambda \gg 1$. For the low shear case, however, this is clearly not the case and the relative emulsion viscosity can exceed the hard sphere limit by a factor of 20. A discussion of this effect will be given in Sec. V.

Next we searched for a way to adequately reproduce the data in Fig. 2 using a minimum number of parameters. This could be done with the following fit functions:

$$\eta_{r,\infty} = \exp\left(\frac{K_1\varphi}{1-\varphi/\varphi_{\max}}\right), \quad \varphi \leqslant \varphi_c, \tag{7a}$$

$$= \exp\left(\frac{K_1\varphi_c}{1-\varphi_c/\varphi_{\max}}\right)\exp[a_3(\lambda+2)(\varphi-\varphi_c)], \quad \varphi > \varphi_c, \tag{7b}$$

$$\eta_{r,0} = \exp[K_\lambda\varphi^{a_1}], \quad \varphi \leqslant \varphi_c, \quad \varphi_c = 0.60, \tag{8a}$$

$$= \exp[K_\lambda\varphi^{a_1}][1+a_2(\varphi-\varphi_c)], \quad \varphi > \varphi_c, \tag{8b}$$

where $K_1 = (2.5\lambda+1)/(\lambda+1)$, $K_\lambda = (10\lambda+8)/(\lambda+1)$, $a_1 = 0.7$, $a_2 = 25$, $a_3 = 0.2$, and $\varphi_{\max} = 1.15$. Finally, the constants in the shear thinning term of Eq. (6) were determined as $k = 0.84$ and $m = 0.8$. Equation (7a) known as the Mooney equation which was shown before to be useful to predict the high shear limit of emulsions [Pal (1992)]. Above a critical volume fraction $\varphi_c = 0.60$ the droplets are in close contact and the interaction mechanism changes. For simplicity, however, we do not introduce a different scaling parameter but simply introduce correction factors above the critical volume fraction [Eqs. (7b) and (8b)]. The results of the fit functions are shown in Fig. 2 as solid lines. For the $\lambda = 1.2$ and 0.1 case the zero shear viscosities could not be determined from the Otsubo data with sufficient accuracy and were therefore omitted in Fig. 2(b). The curves for the fit functions at these viscosity ratios were obtained by comparison with other data sets.

B. The yield stress term

For high volume fractions the drops are in constant contact and form a network of polyhedrally deformed drops. Emulsions of these concentrations do not flow below a certain stress value, termed the yield stress, τ_y. Above that stress value the viscosity is governed by the capillary pressure in the interdroplet gaps. Princen and Kiss (1985, 1986) performed careful measurements on well stabilized $\lambda = 22$ emulsions and observed that this yield stress indeed scaled with σ/a and could be fitted to the semiempirical relation,

$$\tilde{\tau}_y = a_{32}\tau_y/\sigma = \varphi^{1/3}[-0.08-0.114\log(1-\varphi)], \quad 0.8 < \varphi < 1, \tag{9}$$

where they used the so-called Sauter mean drop radius $a_{32} = \Sigma n_i a_i^3/\Sigma n_i a_i^2$ to account for polydispersity effects. More recently, Mason et $al.$ (1996) provided an extensive set of yield stress data for concentrated monodisperse emulsions with a viscosity ratio of 12, which compared well with the results of Princen and co-workers (see Fig. 3). It appeared, however, that the empirical function,

$$\tilde{\tau}_y = C(\varphi-\varphi_y)^2, \quad \varphi_y < \varphi < 1, \tag{10}$$

with $\varphi_y = 0.62$ and $C = 0.51$ gave a much better fit than the Princen equation [Eq. (9)]. From the agreement between the Princen data and that of Mason et $al.$ it is usually tacitly assumed that the yield stress relation is independent of the viscosity ratio. New data for smaller viscosity ratios [$\lambda = 0.4$, Jager-Lézer et $al.$, (1998), and $\lambda = 1.5$, Pal (1999)], however, showed that the yield stress increased with a decrease in the viscosity ratio (see Fig. 3). The reason for this is not clear. In fact, due to the larger degree of deformation and the broader size distribution we would have expected lower yield stress. At this point we just assume that all the data sets are correct and that the yield stress can be approximated by Eq. (10) with a viscosity ratio dependent C and φ_y which are of the form
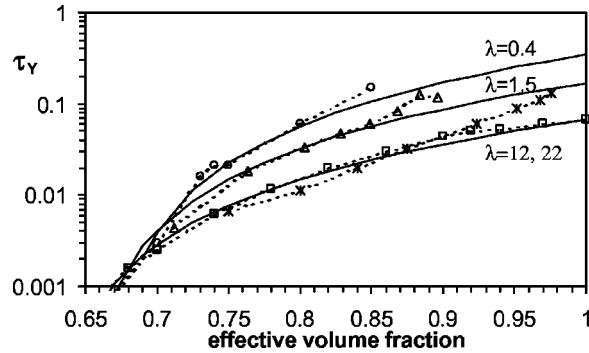
FIG. 3. Dimensionless yield stress as a function of the volume fraction. Open symbols are data of Princen and Kiss; ($\times$) is data of Mason *et al.* (1996); full lines are Eqs. (10) and (11).

$$C(\lambda) = c_0 \frac{\lambda + c_1}{\lambda + c_2}, \quad \varphi_y(\lambda) = b_0 \frac{\lambda + b_1}{\lambda + 1}, \tag{11}$$

with $c_0 = 0.4$, $c_1 = 4.2$, $c_2 = 0.2$, $b_0 = 0.62$, and $b_1 = 1.1$. Note that, although the variation of φ_y with λ is small, a model with a constant φ_y resulted in a significantly poorer fit. The results of this correlation model are shown in Fig. 3 as solid lines.

C. Comparison with different data sources

We will now compare the viscosity predictions as given by the above correlation function with viscosity data available in the literature. We restricted ourselves to studies of emulsion systems that are well characterized in terms of volume fraction, drop size, and surfactant concentration and which precautions were taken to correct or eliminate wall slip. The polydispersity of these emulsion systems was always between 10% and 20%. Data ranges in which drop breakup was reported were not taken into account. The micelle sizes needed for the viscosity predictions were taken from Table I unless otherwise indicated.

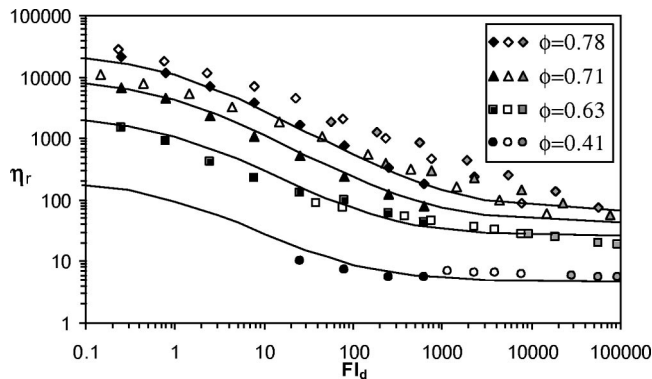In Fig. 4 we plot the data sets given by Pal (1997) versus the depletion flow number

FIG. 4. Data of Pal (1997) for a $\lambda = 29$ oil-in-water emulsion stabilized with 2 wt % Triton X-100. Open symbols: Coarse emulsions ($a = 16$–$32\ \mu$m); gray closed symbols: Fine emulsions ($a \simeq 3.2\ \mu$m); black closed symbols: Corresponding Otsubo data (with $\lambda = 25$); solid lines: predictions according to Eqs. (6)–(8). The contribution of yield stress was not taken into account.
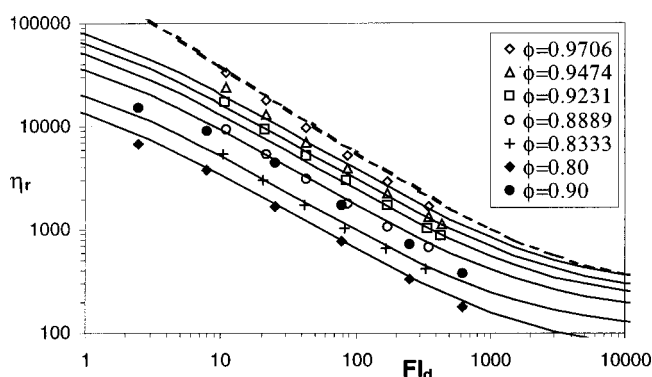
FIG. 5. Viscosity data for extremely highly dispersed phase fractions (the foam limit). Open symbols: Data of Princen and Kiss (1989) for a paraffin oil-in-water system with a viscosity ratio of 32 ($a_m = 27$ Å, estimated); closed symbols: data of Otsubo and Prud'homme (1992); solid lines: predictions without yield stress; dashed line: prediction for the highest phase fraction with the yield stress term.

at four different volume fractions. As expected, the viscosity curves for coarse (open symbols) and fine (gray closed symbols) are superimposed. Most interesting is that the data sets of Otsubo and Prud'homme (1992) agree reasonably well with Pal's data. This may be regarded as remarkable since, although the Otsubo and Prud'homme emulsions have similar physical parameters ($\lambda = 25$ and $\varphi = 0.4$–0.8), the chemical compositions of the fluids and of the emulsifier are completely different. The solid lines are the predictions according to Eqs. (6)–(8). In order to test the usefulness of our model in the limit of $\varphi \to 1$ (the foam limit) we replotted the data of Princen and Kiss (1989) for $\lambda = 32$ emulsions with volume fractions between 0.833 and 0.976 (see Fig. 5). For comparison the data series at $\varphi = 0.80$ and 0.90 of Otsubo and Prud'homme (1992) are also given (closed symbols). The yield stresses for $\varphi < 0.90$ reported by Princen and Kiss for some reason are much lower than those presented in Fig. 3. We therefore chose to present the fit functions *without* the yield stress term (solid lines in Fig. 5). The effect of the yield stress term can be seen by comparing the dashed line in Fig. 5 with the last solid line. For this high volume fraction the yield stress prediction agrees much better with the value reported by Princen and Kiss. This is probably the reason why in this case our model (with the yield stress term) gives a nearly perfect prediction for the emulsion viscosity.

In Fig. 6 the viscosity curves of petroleum ether in water with 0.2 wt % Triton X-100 [Pal (1992)] are compared with the Otsubo and Prud'homme viscosity curves that have a similar viscosity ratio (8.2 vs 6.4 for Pal's data). Note that the solvent viscosity of the Otsubo and Prud'homme data is a factor of 8 larger than that of Pal's data. Apart from Pal's data at a volume fraction of 0.70 all series compare well with the predictions (shown by solid lines).

Next we consider the recent data of Pal (1999) for an oil-in-water emulsion with $\lambda = 1.5$ at relatively high volume fractions. In this case all emulsions were reported to have yield stress. As can be seen from Fig. 7, the predictions [with the yield stress given by Eq. (10)] agree excellently with the data. Further, the Otsubo and Prud'homme data for a system with a similar viscosity ratio (closed symbols) show a perfect overlap with Pal's data.

Finally, in Fig. 8 we present viscosity measurements of a water-in-petroleum oil emulsion with 4 wt % Emsorb 2503 (sorbitan trioleate) as an oil soluble surfactant [after Pal
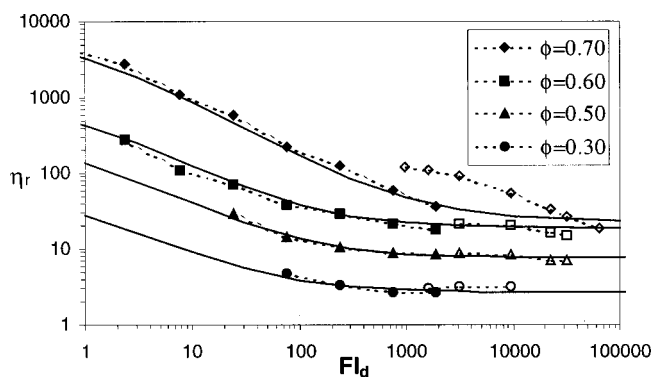
FIG. 6. Combined graph of data of Otsubo and Prud'homme (1992) data (closed symbols, $\lambda = 8.2$) and of Pal (1992) (open symbols, $\lambda = 6.4$; petroleum ether in water $+0.2$ wt % Triton X-100, $\sigma = 0.77$ mN/m). Solid lines are predictions according to Eqs. (6)–(8).

(1996)]. The viscosity ratio was $\lambda = 0.17$, whereas the micelle size was estimated as 25 Å, based on the micelle data for other oil soluble surfactants. Viscosity data corresponding to shear rates below $10^{-3}\,\mathrm{s}^{-1}$ were omitted since it is questionable if these were performed in steady state. The overlap between the viscosity curves of fine emulsions (open symbols) and coarse emulsions (closed symbols) confirms $\dot{\gamma}a^2$ scaling. The predictions for this low viscosity ratio system (solid lines) are not as good as those in the previous comparisons, but the difference with the measurements is at most a factor of 2. The deviations can partly be ascribed to uncertainty of the micelle size. A higher a_m/ϕ_m ratio will shift the yield stress independent part of the predictions to the right, which will improve at least part of the predictions. Note that the part of the viscosity curves where the yield stress predominates ($Fl_d < 100$ for the $\varphi = 0.65$ and 0.76 curves) appears to be correctly predicted.
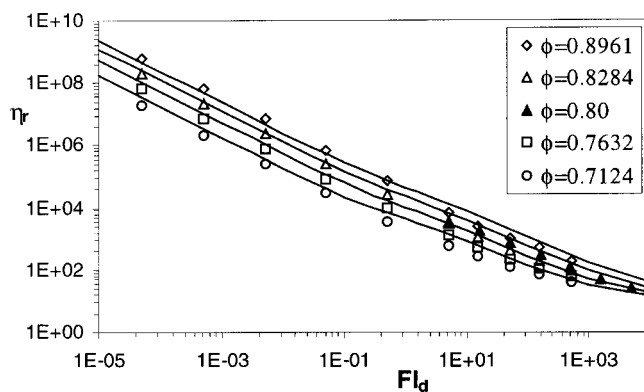

FIG. 7. Data of Pal (1999) for a $\lambda = 1.5$ oil-in-water system at high volume fractions. The emulsions are stabilized with 5.58 wt % Triton X-100. The drop size and interfacial tension reported are $a_{32} = 1.4\,\mu$m and $\sigma = 0.77$ mN/m. Closed symbols: Otsubo data for a $\lambda = 1.5$ system at $\varphi = 0.80$, solid lines: predictions according to Eqs. (6)–(8) and (10).
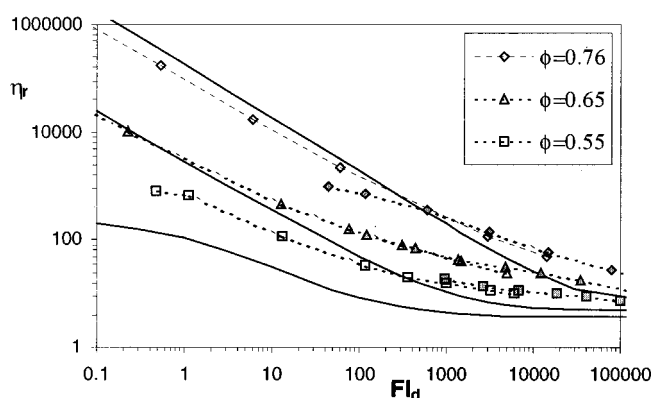
FIG. 8. Data of Pal (1996) for a $\lambda = 0.17$ water-in-oil system stabilized with 4 wt % Emsorb 2503. Open symbols: Fine emulsions (2–6 μm); closed symbols: coarse emulsions (12–15 μm); solid lines: predictions according to Eqs. (6)–(8) and (10). The micelle size was estimated as 25 Å.

V. DISCUSSION

In this article we explored the hypothesis that the depletion flow number is an important scaling parameter for emulsion viscosity. The first confirmations of this idea already appeared from a homologous data series in which systematically the surfactant concentration was varied (Fig. 1). More evidence for Fl_d scaling was shown in Figs. 4–7 where viscosity curves from different studies and with different systems but with similar λ and φ values were shown to overlap when plotted versus Fl_d. We want to note that these overlaps exist even for systems with surfactants of different natures (nonionic Triton X-100 surfactant in most of Pal's systems and anionic Alipal in the Otsubo and Prud'homme data).

Based on a depletion flow number, we developed an empirical model for the viscosity of surfactant stabilized emulsions. As can be seen in Figs. 4–8, this model compares well with all data series for viscosity ratios above about 1. For the lowest viscosity ratio (Fig. 8) the comparison is still reasonable but depends largely on the correctness of the yield stress term. As was mentioned before, some of the observed deviations could be caused by uncertainties in the micelle size but it is clear that the $\lambda \div 1$ limit requires more study.

The physical interpretation of the high shear viscosity plateau, $\eta_{r,\infty}(\varphi,\lambda)$, is relatively well understood. The idea is that at high shear rates all droplet aggregates are destroyed, resulting in an emulsion consisting of separate drops. For such systems the flow properties can be calculated in the low volume fraction limit: $\eta_{r,\infty} = 1 + K_1\varphi$ [Taylor (1932)]. This relation can be extended to higher volume fractions, resulting in the so-called Mooney equation [see, for example, Pal (1992)]. Equation (7a) therefore has the correct limits for $\lambda \neq 1$ as well as for $\varphi \div 0$. For the zero shear viscosity, $\eta_{r,0}(\varphi,\lambda)$, unfortunately no such models are available. Moreover, the zero shear viscosity of emulsions appears to be an order of magnitude larger than that of nonflocculated hard spheres [cf. to the gray line in Fig. 2(b)]. Similar observations were reported by Pal (1999) for emulsions and by Buscall *et al.* (1993) for weakly flocculated solid spheres. The general idea is that this is caused by floc formation. At low shear rates and low volume fractions, large, relatively open aggregates are assumed to be present. The continuous phase within the aggregates is immobilized, which increases the effective volume fraction and thus the viscosity. The convex shape of the measured viscosity data in Fig. 2(b) can be explained by interaction between aggregates. This interaction reduces the average aggregate size

and thus slow down the viscosity increase. The zero shear viscosity equation, proposed in Eq. (8a), is, however, purely empirical.

For the dimensionless yield stress, $\tilde{\tau}_y$, several semiempirical models exist [see, e.g., Princen and Kiss (1989); Reinelt and Kraynik (1989)] none of which includes the effect of the viscosity ratio, λ. An explanation for the observation that the yield stress increases with a *decreasing* viscosity ratio cannot be given at present and it is obvious that this subject deserves more study. In particular, homologous data sets consisting of systems with similar surfactant formulations but different viscosity ratios would be welcome to verify empirical Eqs. (10) and (11).

VI. CONCLUSION

Based on a careful analysis of various viscosity studies available in the literature, we found that the emulsion viscosity must scale proportionally to $\eta_s \dot{\gamma} a^2 \phi_m^{-1}$. We therefore proposed the depletion flow number, $Fl_d = 4\pi \eta_s \dot{\gamma} a^2 a_m / kT \phi_m$, as the corresponding dimensionless parameter for emulsion viscosity. Next it was demonstrated that plots of the relative emulsion viscosity versus the depletion flow number resulted in the overlap of data for systems with different components and different surfactants but with similar volume fraction and viscosity ratio. Finally, it was shown that almost all viscosity data for surfactant stabilized emulsions could be accurately predicted using a simple empirical model. Since this model does not need additional fit parameters, it may be used as a line of reference for new experimental studies.

ACKNOWLEDGMENT

References

Abou-Nemeh, I. and H. J. Bart, ''Microstructures in the system water/D2EHPA/Span-80/*n*-dodecane,'' Langmuir **14**, 4451–4459 (1998).

Amararene, A., M. Gindre, J.-Y. Le Huerou, W. Urbach, D. Valdez, and M. Waks, ''Adiabatic compressibility of AOT reverse micelles,'' Phys. Rev. E **61**, 682–689 (2000).

Aronson, M. P., ''The role of free surfactant in destabilizing oil-in-water emulsions,'' Langmuir **5**, 494–501 (1989).

Asakura, S. and F. Oosawa, ''Interaction between particles suspended in solutions of macromolecules,'' J. Polym. Sci. **33**, 183–191 (1958).

Bibette, J., ''Depletion interactions and fractionated crystallization for polydisperse emulsion purification,'' J. Colloid Interface Sci. **147**, 474–478 (1991).

Buscall, R., J. I. McGowan, and A. J. Morton-Jones, ''The rheology of concentrated dispersions of weakly attracting colloidal particles with and without slip,'' J. Rheol. **93**, 621–641 (1993).

Forland, G. M., J. Samseth, M. I. Gjerde, H. Hoiland, A. O. Jensen, and K. Mortensen, ''Influence of alcohol on the behavior of sodium dodecylsulfate micelles,'' J. Colloid Interface Sci. **203**, 328–334 (1998).

Glatter, O., G. Fritz, H. Lindler, J. Brunner-Popela, R. Mittelbach, R. Strey, and S. U. Egelhaaf, ''Nonionic micelles near the critical point: Micellar growth and attractive interaction,'' Langmuir **16**, 8692–8701 (2000).

Huibers, D. T., V. S. Lobanov, A. R. Katritzky, D. O. Shah, and M. Karelson, ''Predictive critical micelle concentration using a quantitative structure-property relationship approach,'' Langmuir **12**, 1462–1470 (1996).

Jager-Lézer, N., J.-F. Tranchant, V. Alard, C. Vu, P. C. Tchoreloff, and J.-L. Grossiord, ''Rheological analysis of highly concentrated w/o emulsions,'' Rheol. Acta **37**, 129–138 (1998).

Jansen, K. M. B., W. G. M. Agterof, and J. Mellema, ''Droplet breakup in concentrated emulsions,'' J. Rheol. **45**, 227–236 (2001).

Krieger, I. M., "Rheology of monodisperse lattices," Adv. Colloid Interface Sci. **3**, 111–136 (1972).

Loewenberg, M. and E. J. Hinch, "Numerical simulation of a concentrated emulsion in shear flow," J. Fluid Mech. **321**, 395–419 (1996).

Mason, T. G., J. Bibette, and D. A. Weitz, "Yielding and flow of monodisperse emulsions," J. Colloid Interface Sci. **179**, 439–448 (1996).

Mondain-Monval, O., F. Leal-Calderon, J. Phillip, and J. Bibette, "Depletion forces in the presence of electrostatic double layer repulsion," Phys. Rev. Lett. **75**, 3364–3367 (1995).

Otsubo, Y. and R. K. Prud'homme, "Flow behavior of oil-in-water emulsions," J. Soc. Rheol., Jpn. **20**, 125–131 (1992).

Otsubo, Y. and R. K. Prud'homme, "Rheology of oil-in-water emulsions," Rheol. Acta **33**, 29–37 (1994a).

Otsubo, Y. and R. K. Prud'homme, "Effect of drop size distribution on the flow behavior of oil-in-water emulsions," Rheol. Acta **33**, 303–306 (1994b).

Pal, R., "Rheology of polymer-thickened emulsions," J. Rheol. **36**, 1245–1259 (1992).

Pal, R., "Viscous properties of polymer-thickened water-in-oil emulsions," J. Appl. Polym. Sci. **49**, 65–80 (1993).

Pal, R., "Effect of droplet size on the rheology of emulsions," AIChE J. **42**, 3181–3190 (1996).

Pal, R., "Scaling of relative viscosity of emulsions," J. Rheol. **41**, 141–150 (1997).

Pal, R., "Yield stress and viscoelastic properties of high internal phase ratio emulsions," Colloid Polym. Sci. **277**, 583–588 (1999).

Penfold, J., E. Staples, I. Tucker, and P. Cummins, "The structure of nonionic micelles in less polar solvents," J. Colloid Interface Sci. **185**, 424–431 (1997).

Phillies, G. D. J. and J. E. Yambert, "Solvent and solute effects on hydration and aggregation numbers of Triton X-100 micelles," Langmuir **12**, 3431–3436 (1996).

Princen, H. M. and A. D. Kiss, "Rheology of foams and highly concentrated emulsions. II. Yield stress and wall effects," J. Colloid Interface Sci. **105**, 150–171 (1985).

Princen, H. M. and A. D. Kiss, "Rheology of foams and highly concentrated emulsions. III. Static shear modulus," J. Colloid Interface Sci. **112**, 427–437 (1986).

Princen, H. M. and A. D. Kiss, "Rheology of foams and highly concentrated emulsions. IV. Shear viscosity and yield stress," J. Colloid Interface Sci. **128**, 176–187 (1989).

Ravey, J. C., M. Buzier, and C. Picot, "Micellar structures of non-ionic surfactants in apolar media," J. Colloid Interface Sci. **97**, 9–25 (1984).

Reinelt, D. A. and A. M. Kraynik, "Viscous effects in the rheology of foams and concentrated emulsions," J. Colloid Interface Sci. **132**, 491–503 (1989).

Rosen, M. J., *Surfactants and Interfacial Phenomena* (Wiley, New York, 1989).

Sato, T., Y. Saito, and I. Anazawa, "Micellar structure and micellar inner polarity of octaethylene glycol *n*-alkyl ethers," J. Chem. Soc., Faraday Trans. 1 **81**, 275–279 (1988).

Schick, M., ed., *Nonionic Surfactants*, Surfactant Science Series (Dekker, New York, 1967).

Shinoda, K., T. Nakagawa, B. I. Tamamushi, and T. Isemura, *Colloidal Surfactants: Some Physicochemical Properties* (Academic, New York, 1963).

Streletzky, K. and D. J. Phillies, "Temperature dependence of Triton X-100 micelle size and hydration," Langmuir **11**, 42–47 (1995).

Suzuki, K., S. Matsumoto, T. Watanabe, and S. Ono, "Non-Newtonian flow of water-in-oil emulsions," Bull. Chem. Soc. Jpn. **43**, 2773–2777 (1969).

Tanford, C., *The Hydrophobic Effect: Formation of Micelles and Biological Membranes* (Wiley, New York, 1980).

Taylor, G. I., "The viscosity of a fluid containing small drops of another fluid," Proc. R. Soc. London, Ser. A **138**, 41–48 (1932).